https://doi.org/10.5194/hess-2022-236
Preprint. Discussion started: 22 July 2022

Hydrology and Earth System Sciences
Discussions
Open Access

Advance prediction of coastal groundwater levels with temporal convolutional network

Xiaoying Zhang[a,b], Fan Dong[a,b], Guangquan Chen[c], Zhenxue Dai[a,b]*

[a] Institute of Intelligent Simulation and Early Warning for Subsurface Environment, Jilin University, Changchun, China
[b] College of Construction Engineering, Jilin University, Changchun , China
[c] Key Laboratory of Marine Sedimentology and Environmental Geology, First Institute of Oceanography, State Oceanic Administration, Qingdao, China
* Correspondence: Zhenxue Dai, dzx@jlu.edu.cn

Highlights

- A TCN-based model was proposed to predict groundwater levels in coastal aquifers
- Tidal, precipitation and groundwater levels were utilized as input data in the networks
- In advance 1- day, 3-, 7- and 15-days groundwater levels were predicted with the highest accuracy of 1 day-lead prediction
- The TCN-based model outperforms the LSTM in accuracy and efficiency in a coastal aquifer

Abstract

Prediction of groundwater level is of immense importance and challenges for the coastal aquifer management with rapidly increasing climatic change. With the development of artificial intelligence, the data driven models have been widely adopted in predicting hydrological processes. However, due to the limitation of network framework and construction, they are mostly adopted to produce only one-time step in advance. Here, a TCN-based model is developed to predict groundwater level variations with different leading periods in a coastal aquifer. The

https://doi.org/10.5194/hess-2022-236
Preprint. Discussion started: 22 July 2022

Hydrology and Earth System Sciences
Open Access
Discussions

historical precipitation and tidal level data are incorporated as input data. The first hourly-monitored ten-month data were used for model training and testing, and the data of the following three months were predicted with 24, 72, 18 and 360 time steps in advance. For one-step prediction of the two wells, the calculated R^2 are higher than 0.999 in the prediction stage. The performance is meanwhile compared with a powerful network in the field of time-series prediction, long short-term memory (LSTM) recurrent network. The corresponding R^2 of the LSTM-based model are 0.996 and 0.998. While the RMSE values of TCN-based model are less than that of LSTM-based model with shorter running times. For the advanced prediction, the model accuracy greatly decreases with the increase of advancing period from 1-day to 3-, 7- and 15-days. Overall, the TCN- and LSTM-based models show great ability to learn complex patterns in advance using historical data within the time series. Considering the simulation accuracy and efficiency, the TCN-based model outperforms the LSTM-based model and has been proved to be a valid localized groundwater prediction tool in the subsurface environment.

Keywords: prediction; Groundwater level; Coastal aquifer; Temporal convolutional networks; Long Short-Term Memory

https://doi.org/10.5194/hess-2022-236
Preprint. Discussion started: 22 July 2022

Hydrology and Earth System Sciences
Discussions

1 Introduction

As the economic development and population escalate in coastal area, the fresh groundwater needs continue to mount, seawater intrusion has post great threat to the availability of portable water resources globally (Baena-Ruiz et al., 2018). In United States, Mexico, Canada, Australia, India, South Korea, Italy and Greece with dense population, numerous coastal aquifers have experienced salinization caused by seawater intrusion (Barlow and Reichard, 2009; Park et al., 2011; Pratheepa et al., 2015). Protection projects such as aquifer replenishment can be constructed to alleviate seawater intrusion by artificially increasing groundwater recharge in the aquifer than what occurs naturally (Abdalla and Al-Rawahi, 2012; Lu et al., 2019). The replenishment programs have been operated in developed area such as Perth, Western Australia, and California, USA (Garza-Díaz et al., 2019). The infrastructure tends to be costly and out of reach for many developing countries. A reliable seawater intrusion monitoring and predicting system with wells is essential and still the most effective method of keeping water chemistry above the seawater interface (Xu and Hu, 2017).

In the past several decades, conventional numerical models have been widely utilized to simulate and predict the groundwater fluctuation dynamics and chemical variations (Batelaan et al., 2003; Dai et al., 2020; Huang et al., 2015; Li et al., 2002). However, the difficulty of acquiring extensive hydrological and geological data and setting reasonable boundaries limits its application on seawater intrusion management. Meanwhile, the method is not suitable to simultaneously adopt updated monitoring

https://doi.org/10.5194/hess-2022-236
Preprint. Discussion started: 22 July 2022

data and produce real-time prediction. Under such circumstances, where data source is scarce, artificial intelligence technology has been proposed in groundwater dynamic prediction. Artificial neutral network (ANN) has been greatly improved and became a robust tool for dealing groundwater problems, where the flow is nonlinear and highly dynamic in nature (Maier and Dandy, 2000). The conventional network model generally has defects such as high computational complexity, slow training speed, and failure in retaining historical information, thus is hardly to be enrolled in the long-term time-series prediction (Cannas et al., 2006; Mei et al., 2017). To solve this problem, researchers upgraded the conventional networks by integrating them with methods like genetic algorithm (Danandeh Mehr and Nourani, 2017; Ketabchi and Ataie-Ashtiani, 2015), singular spectrum (Sahoo et al., 2017), and wavelet transform (Gorgij et al., 2017; Seo et al., 2015; Zhang et al., 2019). Singular spectrum analysis and wavelet transform can help to preprocess the time-series data before they are put into the neural networks to improve prediction accuracy and efficiency.

With the computing capacity development, deep learning (DL) has emerged as a very powerful time-series prediction method. DL models are particularly suitable for big data time-series, because they can automatically extract complex patterns without feature extraction preprocessing steps (Torres et al., 2019). However, the general fully connected networks are not effective to capture the temporal dependence of time-series (Senthil Kumar et al., 2005). Therefore, more specialized DL models, such as recurrent neural networks (RNN) (Rumelhart et al., 1986) and convolutional neural networks (CNN) (Lecun et al., 1998) have been adopted in the field of time-series

https://doi.org/10.5194/hess-2022-236
Preprint. Discussion started: 22 July 2022

prediction (Feng et al., 2020). Different from the back-propagation (BP) neural network, the RNN preserves the information from the previous step as input to the current step with loops (Coulibaly et al., 2001). This allows the RNN to handle time-series and other sequential data but generally is not straightforward for a long-term calculation in practice (Bengio et al., 1994). Therefore, the enhanced RNN model, long short-term memory (LSTM) is proposed and capable to process high variable-length sequences even with millions of data points (Fischer and Krauss, 2018; Kratzert et al., 2019) . As one of the best deep neural network model in time-series predicting, the LSTM has been widely used in the prediction of temporal variations such as stock market predictions (Fischer and Krauss, 2018), rainfall-runoff (Kumar Dubey et al., 2021) and groundwater level (Solgi et al., 2021). Despite of substantial progresses in hydrology predicting, these networks still have issues of low training efficiency and low accuracy (Zhan et al., 2022).

More recently, a variant of the CNN architecture known as temporal convolutional networks (TCN) has acquired popularity (Bai et al., 2018). The prominent characteristic of TCN is its ability to capture long-term dependencies without information loss (Cao et al., 2021). Meanwhile, it joints a residual block structure to fix the disappearance of gradient in the deep network structure (Chen et al., 2020). With proper modifications, the TCN is quite genetic and easily to be used to build a very deep and extensive network in sequence modeling. In earth science, the TCN has been successfully applied to time-series prediction tasks including multivariate time-series predicting for meteorological data (Wan et al., 2019),

https://doi.org/10.5194/hess-2022-236
Preprint. Discussion started: 22 July 2022

probabilistic predicting (Chen et al., 2020) and wind speed predicting (Gan et al., 2021). Researches suggest that the TCN convincingly has advantage in several popular deep learning models across a broad range of sequence modeling tasks (Borovykh et al., 2019; Chen et al., 2020; Wan et al., 2019). However, the potential of TCN has not been investigated in the sequencing model of hydrogeology field.

Another import subject is that these networks are mostly used to predict variables in only one step, which is not enough for the prediction of hydrology information in management. Therefore, it is worthy to explore their prediction abilities in longer periods. The objective of this study is to build a climate-dydro hybrid data-driven model with TCN to develop a real-time advance prediction model of groundwater level in the coastal aquifers. The hourly processed tidal, precipitation with groundwater level data in monitoring wells of Laizhou Bay are utilized to train model and prediction the groundwater level in a period of 1-day, 3-,7- and 15-days. To further validate the accuracy and efficiency of the proposed model, its performance is further compared with the LSTM-based model. The rest of the paper is organized as follows. Sect. 2 introduces the study area and observational data. Sect. 3 illustrates the detailed concept of TCN and LSTM, the experimental model settings and model evaluation criteria. Sect. 4 presents the predicting results and discussions. Finally, the paper is concluded in Sect. 5.

2 Study area and data processing

2.1 Site description

The study area is located in the south coast of Laizhou Bay, along the Yangzi to

https://doi.org/10.5194/hess-2022-236
Preprint. Discussion started: 22 July 2022

Weifang section in Shandong province of China (Fig. 1). The Laizhou Bay is one of the earliest and most seriously affected area by seawater intrusion since 1970s in China (Han et al., 2014; Zeng et al., 2016). The area is basically a coastal plain, which contains a series of Cretaceous to modern sediments that covering the Paleozoic basement. The sedimentary facies of coastal aquifer are alluvium, proluvial and marine sediments from south to north (Han et al., 2011). According to the research of (Xue et al., 2000), there have been three seawater intrusion and regression events in the sea area of Laizhou Bay since the upper Pleistocene. The transgression in the early upper Pleistocene formed the third marine aquifer containing sedimentary water. These brine were formed by evaporation and concentration of ancient seawater and re-dissolution and mixing of salt (Dai and Samper, 2006; Zhang et al., 2017). The monitoring wells BH01-BH05 are distributed in the study area along a cross section perpendicular to the coastline. Among the wells, the data of well BH01 and BH05 are relatively integrate and distributed in the two sides of the cross profile with distinguished annual variation pattern, which are selected as examples for the developed models.

https://doi.org/10.5194/hess-2022-236
Preprint. Discussion started: 22 July 2022

Figure 1. Schematic figure of the study area with monitoring wells BH01-BH05.

2.2 Data collection and preprocessing

The precipitation and tidal level are selected as the primary factors to affect the groundwater dynamics in the coastal area. The data in the period of 2011 to 2012 with groundwater level observations of three wells are combined as the input of the deep learning models. A total of 37,920 data items are collected for monitoring wells and the variations of groundwater level, and tidal level with precipitation are shown in Figure 2. The rainfall is concentrated from June to September and in shortage from December to April. The tide in the study area is irregular mixed with a semi-diurnal variation. In the experiments, ten months of data from October to July 2011 is first extracted for model training and testing. The rest of the data from August 2012 to October 2012 is used to test model prediction accuracy.

In addition, the magnitudes of meteorological and hydrological variables have

https://doi.org/10.5194/hess-2022-236
Preprint. Discussion started: 22 July 2022

Hydrology and Earth System Sciences
Discussions
Open Access

obvious temporal variations. To reduce the negative impact on the model learning ability, especially on the speed of gradient descent, all variables are normalized to ensure that they remain at the same scale (Kratzert et al., 2019). This preprocessing method ensures the stable convergence of parameters in the developed TCN- and LSTM-based models and improve the simulation accuracy of the model. The normalization formula is as follows:

$$y_i = \frac{x_i - x_{min}}{x_{max} - x_{min}} \tag{1}$$

where x_i represents the data in time i; x_{max} and x_{min} are the maximum and minimum variable values. The output of the network is retransformed to obtain the final groundwater level prediction, which is an inverse data scaling process.

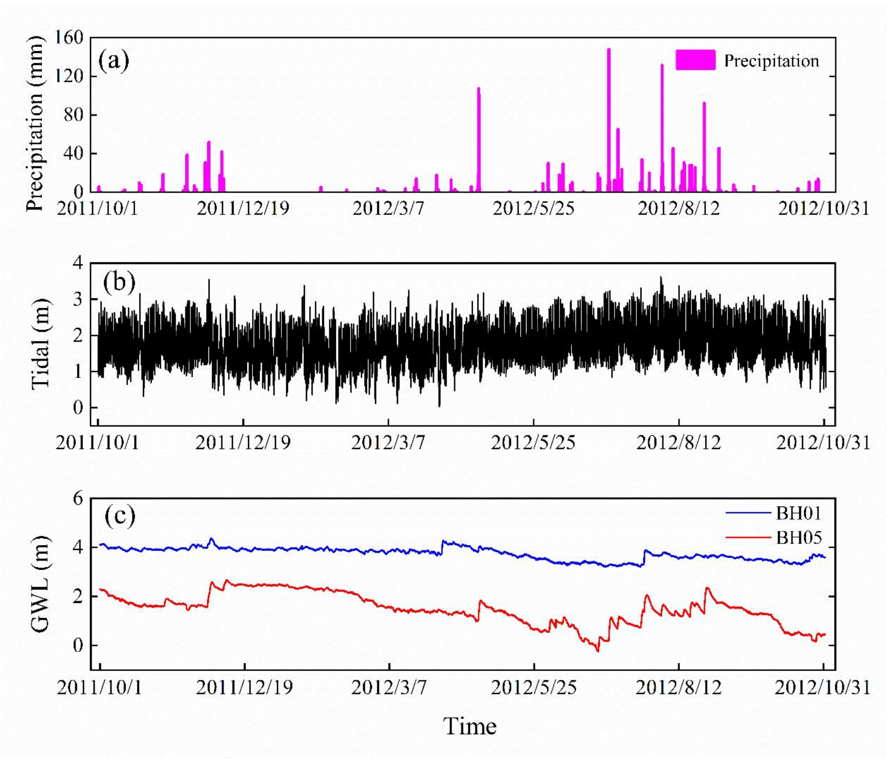

https://doi.org/10.5194/hess-2022-236
Preprint. Discussion started: 22 July 2022

Figure 2. Time-series of the variables in the study, including (a) precipitation, (b) tide, (c) groundwater level (GWL).

3 Methodology

3.1 Temporal Convolutional Network (TCN)

The TCN is first proposed by (Lea et al., 2016) for video action segmentation and detection by hierarchically capturing intermediate feature presentations. Then the term is extended for sequential data for a wide family of architectures with generic convolution (Bai et al., 2018; Lea et al., 2017). Suppose that we have an input hydro-climate sequence at different times x_0, ..., x_T, the goal of the modeling is to predict the corresponding groundwater level as outputs y_0, ..., y_T at each time. The problem could transfer to build a network f that minimizes the function loss between observations and actual network outputs $L[(y_0, ..., y_T),(\hat{y}_0,..., \hat{y}_T)]$, where $\hat{y}_0,..., \hat{y}_T = f(x_0, ..., x_T)$. Currently, a typical TCN consists of dilated, causal 1D full-convolutional layers with the same input and output lengths. With TCN, the prediction y_t depends only on the data from x_0 and x_t and not include the future data from x_t and x_T (Yan et al., 2020). With the three key components of TCN, it has two distinguishing characteristics: 1) the TCN is able to map the same length of output as the input sequence as in RNN; 2) the convolution involved in TCN is causal, eliminating the influence of future information on the output.

3.1.1 Causal Dilated Convolutions

In the TCN, the first advantage is accomplished by a 1D full-convolutional network (FCN) architecture. Different from the traditional CNN, the FCN transforms

https://doi.org/10.5194/hess-2022-236
Preprint. Discussion started: 22 July 2022

the fully connected layers into the convolutional layers for the last layers, preserving the same length of output as that of the input (Long et al., 2015). As shown in Fig. 3a, the lengths of the input, the hidden and the output layers are the same in the FCN. Some zero padding is needed in this step by adding additional zero-valued entries with a length of kernel size-1 in each layer. The kernel size is the number of successive elements that are used to produce one element in the next layer.

To avoid the information leakage from the future (after time *t*), the TCN uses causal convolution instead of standard convolution, where only the elements at or before time *t* in the previous layer are adopted into the mapping of the output at time *t*. Further, the dilated convolution is employed to capture long-term historical information by skipping a given step size (dilation factor *d*) in each layer. For example, the dilation factor *d* increases from 1 to 4 with the evolution of the network depth (*n*) in an exponential increasing pattern. In this way, a very large receiving domain is created and all the historical records in the input can be involved in the prediction model with a deep network.

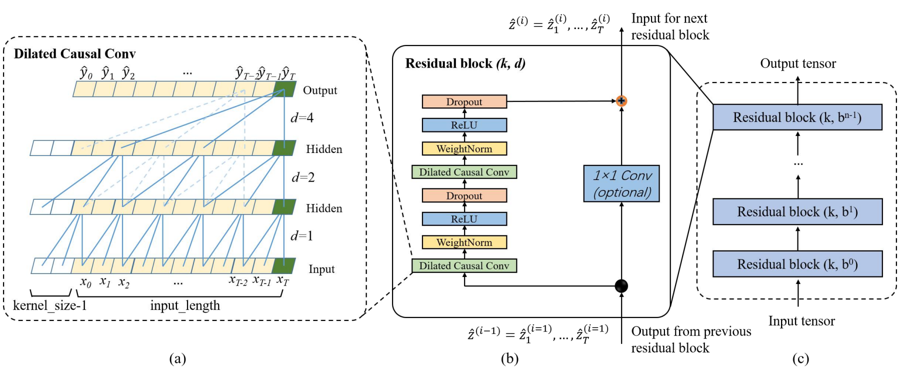

Figure 3. Architectural elements in the proposed TCN. (a) the structure of causal

https://doi.org/10.5194/hess-2022-236
Preprint. Discussion started: 22 July 2022

dilated convolution; (b) the TCN residual block. An 1x1 convolution is added when residual input and output have different dimensions; (c) framework of residual connection in the TCN.

3.2.2 Residual Connections

In a high dimensional and long-term sequence, the network structure could be very deep with increasing complicity and cause a vanishing gradient. To solve this issue, a residual block structure is introduced to replace the simple 1D causal convolution layer, so that the designed TCN structure is more generic (He et al., 2016). The residual block in a TCN is represented in Fig. 3b. It has two convolutional layers with the same kernel size and dilation factor and non-linearity. To solve non-linear models, the rectified linear unit (ReLU) is added to the top of the convolutional layer (Nair and Hinton, 2010). The weight normalization is applied between the input of hidden layers (Salimans and Kingma, 2016). Meanwhile, a dropout is added after each dilated convolution for regularization (Srivastava et al., 2014). For all connected inner residual blocks, the channel widths of input and output are consistent. But the width may be different between the input of the first convolutional layer of the first residual block and the output of the second convolutional layer of the last residual block. Therefore, a 1×1 convolution is added in the first and last residual block to adjust the dimensions of the residual tensor into the same. The output of the residual block is represented by $\hat{Z}^{(i)}$ for the i^{th} block.

3.2.3 Structure of TCN

A complete structure of TCN is illustrated in Fig.3c. It contains a series of proceeding residual blocks. The structural characteristics make TCN a deep learning network model very suitable for complex time-series prediction problems (Lara-Benítez et al., 2020). The main advantage of TCN is that, similar to RNN, they have flexible receptive fields and can deal with various length input by sliding one-dimensional causal convolution kernel. Furthermore, because TCN shares a convolution kernel and has parallelism, it can process long sequences in parallel instead of sequential processing like RNN, so it has lower memory usage and shorter computing time than a cyclic network. Moreover, RNN often has the problems of gradient disappearance and gradient explosion, which are mainly caused by sharing parameters in different periods, while TCN uses a standard backpropagation-through-time algorithm (BPTT) for training, so there is little gradient disappearance and explosion problem (Pascanu et al., 2012). The detailed mathematical calculation and associated information of the TCN architecture are referred to (Bai et al., 2018).

3.2 Long Short-Term Memory network (LSTM)

LSTM is a special RNN model explicitly designed for long-term dependence problems. As shown in Fig. 4a, the RNN has a series of repeating modules that recursively connected in the evolution direction of the sequence. The chain-like structure permits the RNN to retain important information in a "tanh" layer and produce the same length of output $\hat{y}_t$ as input x_t. However, the short-length "remember time" is not enough for the groundwater prediction. Especially for our hourly recorded data, a maximum step about ten reported by (Bengio et al., 1994) is unable to count the effect of annually, seasonally, and even daily groundwater

https://doi.org/10.5194/hess-2022-236
Preprint. Discussion started: 22 July 2022

Hydrology and Earth System Sciences
Open Access
EGU
Discussions

variation. Different from the simple layer in the RNN, the LSTM has a more complicated repeating module with four interacting layers.

The core idea of LSTM is the special structure to control the cell state in the module as shown in Fig.4b. It includes a cell and an input gate i_t , a forget gate f_t, and an output gate o_t. The information can directly flow down along cells C without critical changes, therefore, preserving long-term history messages (Zhang et al., 2018b). The three gates control which data in a sequence is important to keep or throw away, and protect the relevant information passed down in the cell to make predictions. The forget gate f_t has a sigmoid layer to determine which information is discarded with a value between 0 and 1. The lower the value, the less the information added to the cell state (Ergen and Kozat, 2018). Opposite the forget gate, the input gate i_t decides what information to retain in the cell state. It is composed of two parts: a sigmoid layer and a tanh layer. The two layers are combined to govern which values will be updated by generating a new candidate value $\tilde{C}_t$. The old cell state C_{t-1} then can be updated into the new cell state C_t with a weighted function. Finally, the output gate o_t determines what parts of the cell state should be passed on to the next hidden state. The detailed calculation of the LTSM can be referenced to (Lea et al., 2016).

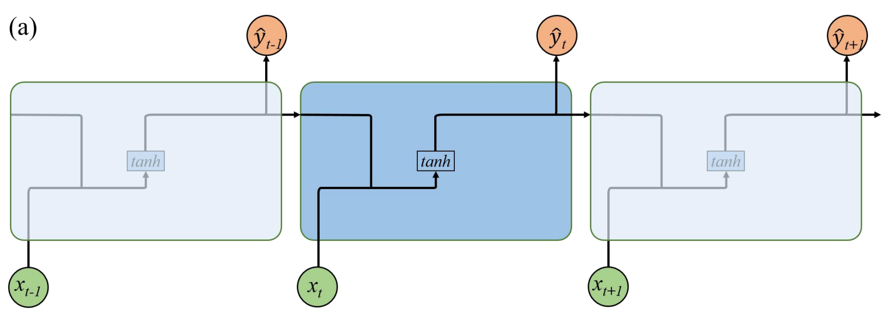

https://doi.org/10.5194/hess-2022-236
Preprint. Discussion started: 22 July 2022

Hydrology and Earth System Sciences
Open Access
Discussions

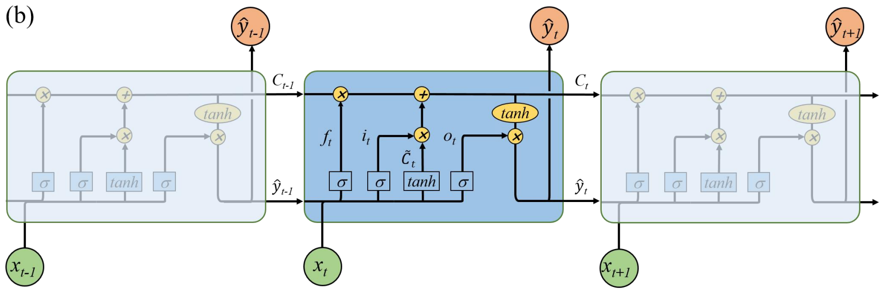

Figure 4. Graphical representation for a) chain like structure of the RNN by assigning x_t and $\hat{y}_t$ as input and output. The self-connected hidden units allow information to be passed from one step to the next; b) LSTM's memory block based on RNN. The hidden block includes three gates (input i_t, forget f_t, output o_t) and a cell state to select and pass the historical information.

3.3 Experimental study

Due to the high complexity of the DL models, setting appropriate hyper-parameters for the developed networks is very important. Here, the impact of the size of the input window, the epoch number and the batch size were tested with different convolutional architectures over the monitoring data (Lara-Benítez et al., 2020). The learning dataset is first divided into two parts: 80% of the time-series data is used as training set, and 20% of the data is utilized as testing set. The effect of different splitting strategies is further tested in section 4. With the increase of the epoch numbers, the curve gradually approaches to the optimal fitting state from the initial non-fitting state, but too many epochs frequently lead to over-fitting of the neural network. Meanwhile, the number of iterations generally increases for updating weights in the neural network. Therefore, the number of epoch from 0 to 300 is evaluated. Batch size represents the number of samples between model weight

https://doi.org/10.5194/hess-2022-236
Preprint. Discussion started: 22 July 2022

updates (Kreyenberg et al., 2019). The value of the batch size often is set between 1 and hundreds. Larger batch size often leads to faster convergence of the model, but may lead to less ideal of the final weight set. To find the best balance between memory efficiency and capacity, the batch size should be carefully set to optimize the performance of the network model. Besides these parameters, the number of filters in the TCN-based and the hidden nodes in the LSTM-based model were as well tested within reasonable ranges.

The 1-day, 3-, 7-, and 15-days lead prediction experiments were further conducted to test the capacity of DL methods in predicting long-term groundwater level in the coastal aquifer. To eliminate the randomness of model training, all experiments were repeated 5 times and the average values of each index were compared. In all experiments, the average absolute error (MAE) has been used as the loss function of networks (Lara-Benítez et al., 2020). The Adam optimizer has an adaptive learning rate, which can improve the convergence speed of deep networks, which has been used to train the models (Kingma and Ba, 2015).

3.4 Evaluation of model performance

Two evaluation metrics, coefficient of determination (R^2) and root mean square error (RMSE) are selected to quantify the goodness-of-fit between model outputs and observations ((Zhang et al., 2020)). The two criteria are calculated using the following equations:

$$RMSE = \sqrt{\frac{1}{N}\sum_{i=1}^{N}(h_i - y_i)^2} \tag{1}$$

$$R^2 = \frac{\sum_{i=1}^{N}(h_i - \bar{h})^2 - \sum_{i=1}^{N}(h_i - y_i)^2}{\sum_{i=1}^{N}(h_i - \bar{h})^2} \tag{2}$$

https://doi.org/10.5194/hess-2022-236
Preprint. Discussion started: 22 July 2022

where h_i is the observed groundwater level at time i, y_i is the network prediction values at time i, $\bar{h}$ is mean of the observed groundwater levels, and n is the number of observations. RMSE measures the prediction precision which creates a positive value by squaring the errors. The RMSE score is between [0, ∞]. If the RMSE approaches to 0, the model prediction is ideal. R^2 measures the degree of model replication results, ranging between [−∞, 1]. For the optimal model prediction, the score of R^2 is close to 1.

4 Results and discussions

4.1 Hyper-parameter trial experiments

4.2.1 Experiments of the TCN-based model

The TCN-based model is built on Keras platform, using TensorFlow of python as the backend. Take the groundwater level dataset in well BH1 as an example, the trials are set up with a variety combination of different hyper-parameters that are set in the TCN-based model as illustrated in Table 1. With the fixed number of epoch, the result of 32 filters is better than that of 16 and 64 filters. Meanwhile, under the condition of 32 filters, the results of the model decrease with the increase of batch size. Therefore, when three different batches of 16, 32, and 64 are set for testing, the results of the 16 batch size of the model are better. Based on the above experimental results, the influence of different numbers of epoch on the simulation is further explored with the filters equals to 32 and the batch size equals to 16 as shown in Fig.5. The overall results of the model are improved when the number of epoch increases from 100 to 190 though the variation is not strictly linear, and the results turn stable with minor

https://doi.org/10.5194/hess-2022-236
Preprint. Discussion started: 22 July 2022

fluctuations when the number of epoch exceeds 200.

Table 1. The RMSE and R^2 values between the observed and predicated groundwater levels in well BH1 with different numbers of epochs, different numbers of filters, and different batch sizes. The bold values represent the optimal hyper-parameters with the smallest RMSE and the highest R^2 scores in the TCN-based model.

Epoch	filters	Batch size	RMSE(m)	R^2	Time(min)
100	32	16	0.0182	0.9904	1.29
		32	0.0117	0.9876	1.05
		64	0.0117	0.9875	0.78
200	16	16	0.0078	0.9946	2.41
		32	0.0068	0.9959	1.75
		64	0.009	0.9942	1.19
200	**32**	**16**	**0.0059**	**0.997**	2.58
		32	0.0075	0.9948	2.01
		64	0.0082	0.9938	1.51
200	64	16	0.0125	0.9906	3.68
		32	0.0101	0.9907	3.21
		64	0.0157	0.9775	2.76
300	32	16	0.0065	0.9955	3.8
		32	0.0076	0.9946	3.01
		64	0.0099	0.9904	2.22

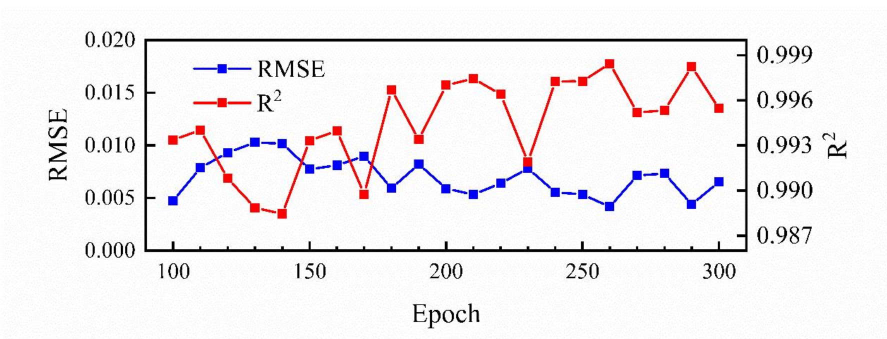

https://doi.org/10.5194/hess-2022-236
Preprint. Discussion started: 22 July 2022

Figure 5. The variation of RMSE and R^2 values between the observed and simulated groundwater levels of well BH1 with the increasing number of epoch when the number of filters is 32 and the batch size is 16.

4.2.2 Experiments of the LSTM-based model

The maximum epoch and the number of hidden nodes are two key parameters affecting the simulation accuracy of LSTMs (Zhang et al., 2018a). Different hyper-parameter combinations are tested as well as in the proposed TCN-based model with groundwater levels in well BH1. The RMSE, R^2 and running time are shown in Table 2. With fixed number of hidden nodes, the results of 100 and 200 epochs are better than that in the 300 epochs experiment. A detailed variation of RMSE and R^2 values with increasing hidden nodes and epoch are further illustrated in Fig. 6. The figure shows that the RMSE and R^2 have a decreasing and increasing trend separately when number of epochs is greater than 150 but they turn to the opposite way when it is larger than 240. The variations of RMSE and R^2 with increasing hidden nodes have similar changes as well. The results indicate that though an insufficient number of neurons may decrease the learning ability of the network, an increasing training hyper-parameters may not ensugare better rFesults.

Table 2. The RMSE and R^2 values between the observed and simulated groundwater levels in well BH1 with different numbers of epochs and hidden nodes. The bold values represent the optimal hyper-parameters used in the proposed LSTM-based model.

Epoch	Hidden nodes	RMSE	R^2	Time(min)
100	50	0.0104	0.9902	1.01

https://doi.org/10.5194/hess-2022-236
Preprint. Discussion started: 22 July 2022

	60	0.0098	0.9916	1.38
	70	0.0095	0.9922	1.53
	80	0.01	0.9913	1.75
200	50	0.0094	0.9922	1.91
	60	0.0089	0.9931	2.59
	70	**0.0088**	**0.9932**	**2.96**
	80	0.0092	0.9925	3.28
300	50	0.0101	0.9903	2.86
	60	0.0105	0.9901	3.85
	70	0.0103	0.9907	4.29
	80	0.0120	0.9872	4.92

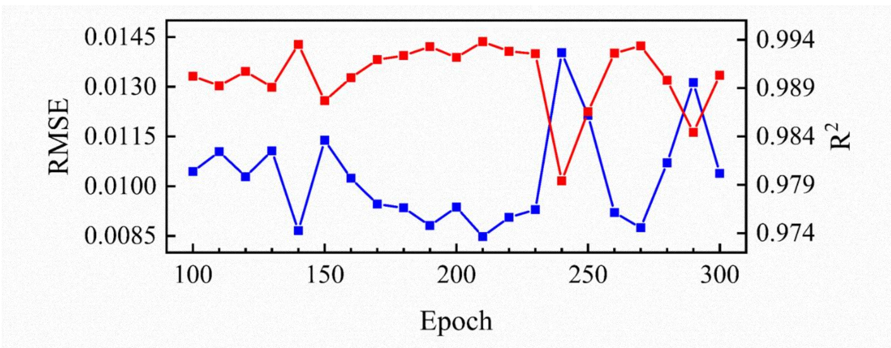

Figure 6. The variation of RMSE and R^2 values between the observed and simulated groundwater levels of well BH1 with the increasing of the number of epochs when the hidden node is 50.

The trial experimental results present similar fitting pattern shared by the two kind of networks. Inadequate hyper-parameters often leads to deficient learning ability of the network. In the contrary, excessive parameter setting may cause neural network overfitting issues. In addition, the growing parameters dramatically increase the computational cost in the network. For example, the time cost from 50 to 80 hidden nodes increased about 1.7 times in each iteration trial in the LSTM-based

https://doi.org/10.5194/hess-2022-236
Preprint. Discussion started: 22 July 2022

model. Therefore, during implementation, 200 epochs, 32 filters, and the 16 batch size were chosen as the optimal parameters in the TCN network. For the LSTM network, the number of epoch and hidden nodes were chosen as 200 and 70.

4.3 Model performance and evaluation

The optimal hyper-parameters of the proposed TCN-based model for groundwater level predicting are shown in Table 1 (epoch = 200, filters = 32 and batch size = 16). Besides that, the kernel size in each convolutional layer is set as 6, the dilations are [1,2,4,8]. For the LSTM-based model, the batch size is set to 148 with epoch=200 and nodes=70. The same hyper-parameters are then utilized to construct TCN and LSTM architectures for prediction of groundwater level in different monitoring wells.

The simulated groundwater level in the training and testing stages by the two models are shown in Fig. 7. For both models, the simulated values completely capture the variation of groundwater levels in monitoring wells with overlapped plot. The R^2 and RMSE values of simulation results are listed in Table 3. For the TCN-based model, the values of RMSE are 0.0019 and 0.0166 for BH1, and the values of R^2 are larger than 0.999 in the prediction. For the LSTM-based model, the RMSE values are 0.0074 and 0.0588, and the R^2 values are 0.9957 and 0.9980. These metrics indicate that both of the models can “remember” the historical records and produce true observations. The simulation accuracy of TCN-based models is slightly higher than the LSTM-based models. In addition, the running time of the TCN-based model is 2.6 minutes, which is faster than that of the TCN-based model by eliminating the gate selection.

https://doi.org/10.5194/hess-2022-236
Preprint. Discussion started: 22 July 2022

Hydrology and Earth System Sciences
Open Access
EGU
Discussions

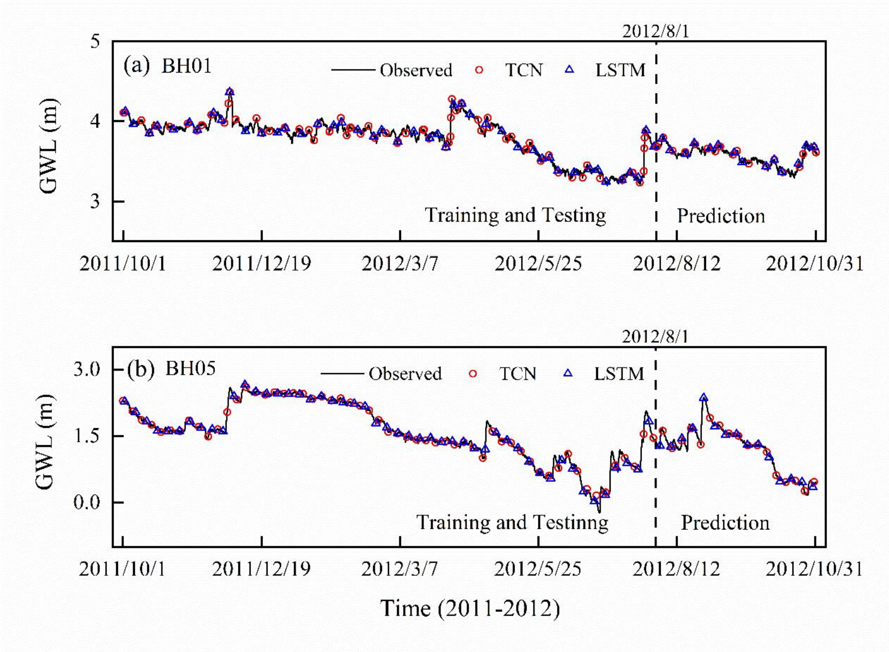

Figure 7. The simulation results of groundwater level of different monitoring wells by TCN-based model. The black dash line divides the data into two groups: the training and testing set.

Table 3. The model results for groundwater level in the training and testing and prediction stage

Well	Model	Training and Testing			Prediction		
		MAE	RMSE	R^2	MAE	RMSE	R^2
BH01	TCN	0.0017	0.0068	0.9992	0.0009	0.0019	0.9997
	LSTM	0.0053	0.0077	0.9990	0.0050	0.0074	0.9957
BH05	TCN	0.0070	0.0279	0.9981	0.0061	0.0166	0.9990
	LSTM	0.0082	0.0116	0.9997	0.0168	0.0558	0.9980

https://doi.org/10.5194/hess-2022-236
Preprint. Discussion started: 22 July 2022

Hydrology and Earth System Sciences
Discussions

4.4 Long term leading time prediction

The TCN- and LSTM-based models were further adjusted to predict the groundwater level of the coastal aquifer over three months ahead with different leading period. Prediction results of groundwater level with 1-day, 3-, 7-, and 15-days leading time of TCN- and LSTM-based models are illustrated in Fig. 8 and Fig. 9 for wells BH1 and BH5 respectively. The results show that the predicted groundwater values in monitoring wells have the same change trend as the actual groundwater level. Both of the models are able to capture the variation trend of groundwater levels in the two monitoring wells.

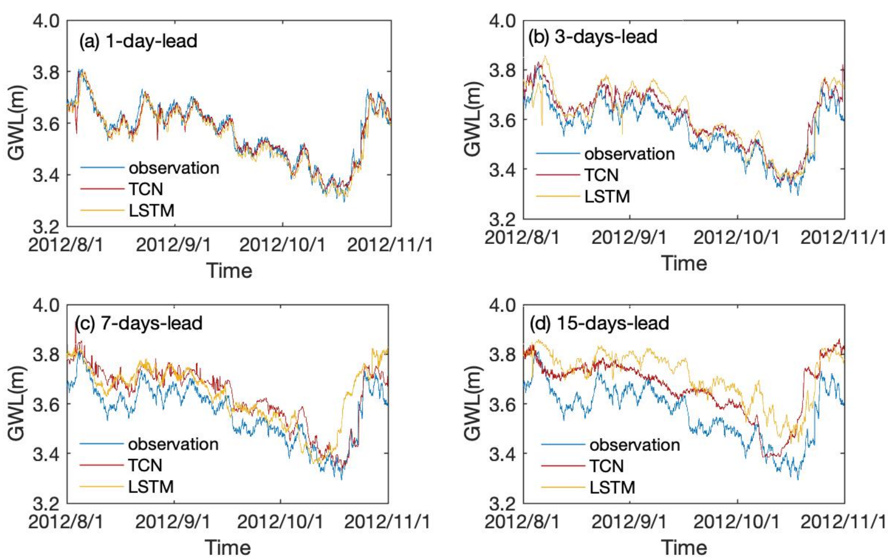

Figure 8. The observed and prediction values of the groundwater level with TCN- and LSTM-based models for 1-day, 3-, 7- and 15-days lead period in monitoring well BH01.

https://doi.org/10.5194/hess-2022-236
Preprint. Discussion started: 22 July 2022

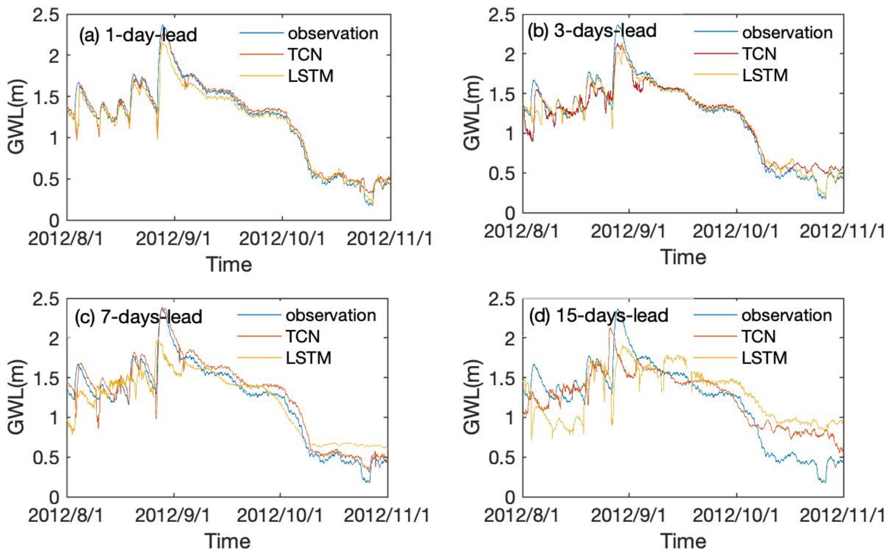

Figure 9. The observed and prediction values of the groundwater level with TCN- and LSTM-based models for 1-day, 3-, 7- and 15-days lead period in monitoring well BH05.

To quantitatively compare the prediction accuracy of the proposed TCN- and LSTM-based models, the results of two evaluation metrics with the model running time in different monitoring wells are summarized in Table 4. It can be learned that the R^2 value of TCN-based models decreased from 0.9386 to 0.1406 for well BH01 and from 0.9670 to 0.7271 for well BH05. Correspondingly, an increase of RMSE values from 0.028 to 0.1209 and 0.0934 to 0.206 are observed for BH01 and BH05, separately. A similar variation pattern is recognized for LSTM-based model with smaller R^2 and higher RMSE than that of the TCN-based model. While, the average running time of TCN-based is about 3.4 seconds, which is about 6 seconds for LSTM-based models.

https://doi.org/10.5194/hess-2022-236
Preprint. Discussion started: 22 July 2022

Hydrology and Earth System Sciences
Open Access
Discussions

Table 4. The model results for groundwater level in the long term prediction

Well	Model	Prediction		Model	Prediction	
		RMSE	R^2		RMSE	R^2
BH01	TCN-1	0.0280	0.9386	LSTM-1	0.0349	0.9047
	TCN-3	0.0550	0.7638	LSTM-3	0.0640	0.6802
	TCN-7	0.0741	0.5713	LSTM-7	0.0956	0.2874
	TCN-15	0.1209	-0.1407	LSTM-15	0.1486	-0.7227
BH05	TCN-1	0.0934	0.9670	LSTM-1	0.1012	0.9613
	TCN-3	0.1375	0.9285	LSTM-3	0.1086	0.9554
	TCN-7	0.1084	0.9296	LSTM-7	0.2050	0.8406
	TCN-15	0.2060	0.7271	LSTM-15	0.3515	0.5330

The results showed that the TCN- and LSTM-based models are able to predict the variation of groundwater levels with longer leading period more than one time step. The performance of the two networks were further evaluated with Taylor diagrams by taking different criteria aspects into account (Taylor, 2001). The comparisons of TCN- and LSTM-based model are shown in Fig. 10. As the metrics distributed away from the reference point (Ref), the deviation of prediction from observation is gradually increased with extending of leading period. Taken well BH01 for example, the prediction with 1-day (24 hours prediction window) in advance are the highest in agreement with the actual situation in the two models. The two simulation results have the lowest RMSE values and highest R^2 values for both models. The prediction precision gradually decreases with the extending of leading time. For the leading time smaller than 7-days, 168 time steps prediction in advance, the evaluation metrics have acceptable values of less than 0.1 for RMSE but the R^2 values have been greatly dropped. For the 15-days (360 time steps) leading period, the RMSE of the TCN- and LSTM-based models have increased to 0.1209 and 0.1486 with negative R^2 values,

https://doi.org/10.5194/hess-2022-236
Preprint. Discussion started: 22 July 2022

which suggest a kind of overestimation in well BH01.

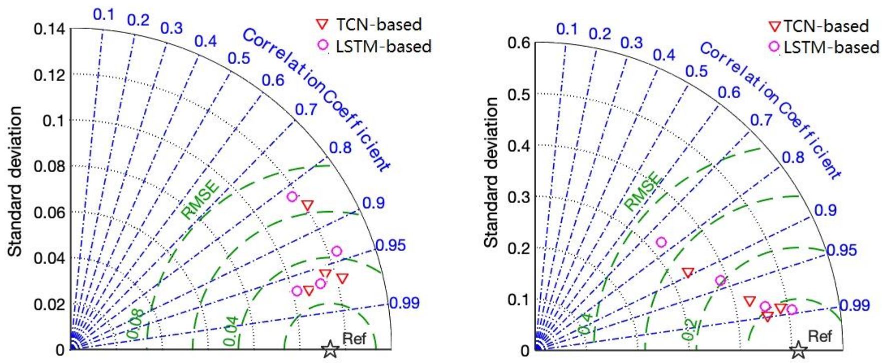

Figure 10. Taylor diagrams with statistical (RMSE, correlation coefficient, and standard deviation) comparison results of the TCN-based and LSTM-based models for well (a) BH01 (b) BH05.

Overall, TCN- and LSTM-based models both have strong prediction ability. The performance of the TCN-based model is better than that of the LSTM-based model in the three months prediction concerning both model precision and running time. However, the model precision decreases when the leading period is increasing. The causal dilated convolutions used by TCNs are better at capturing long-term dependencies of time series data than recurrent units, improving the efficiency of neural networks and shortening the network running time. The TCN-based models are able to provide accurate predictions once they are trained. As expected, the processing speed of parallel convolution TCN-based models for long input sequences is faster than that of recurrent networks. This seems to be a basic advantage of real-time monitoring and early warning. In real-time monitoring and early warning, it is necessary to obtain predictions quickly to make wise decisions.

https://doi.org/10.5194/hess-2022-236
Preprint. Discussion started: 22 July 2022

4.5 Influence of training set percentage

In the following section, we discuss the similarities and differences between TCN- and LSTM-based in terms of training set percentage. As we all know, data-driven methods are supported by data; however, how much data is needed to build an effective model is still a problem. This is because specific problems depend on application cases, data features, and model features (Wunsch et al., 2021). In our study, the data is the hourly-monitored data from 2011 to 2012. From 2011, we set 20%, 30% to 90% training sets in turn, so as to gradually expand the length of training set.

Fig. 11 shows the effect of increasing the percentage of training set on the performance of the model. All experiments were repeated five times, and the average values of each index were compared to make them comparable. We observed that the overall performance of the TCN-based model improved with the increase of the percentage of training set. When the training set reached 80%, the performance was relatively optimal, and then the performance began to deteriorate with the increase of the percentage of training set; at the same time, it can be seen that the performance of the LSTM-based model tends to be stable when the training set reaches 70%, and then decreases slightly with the increase of training set. Therefore, it is not that the more training sets, the better the performance of the model. We should carefully evaluate and shorten the training data set as much as possible when necessary. Finally, we set 80% of the training set length to simulate the coastal aquifer time-series data.

https://doi.org/10.5194/hess-2022-236
Preprint. Discussion started: 22 July 2022

Hydrology and Earth System Sciences
Discussions

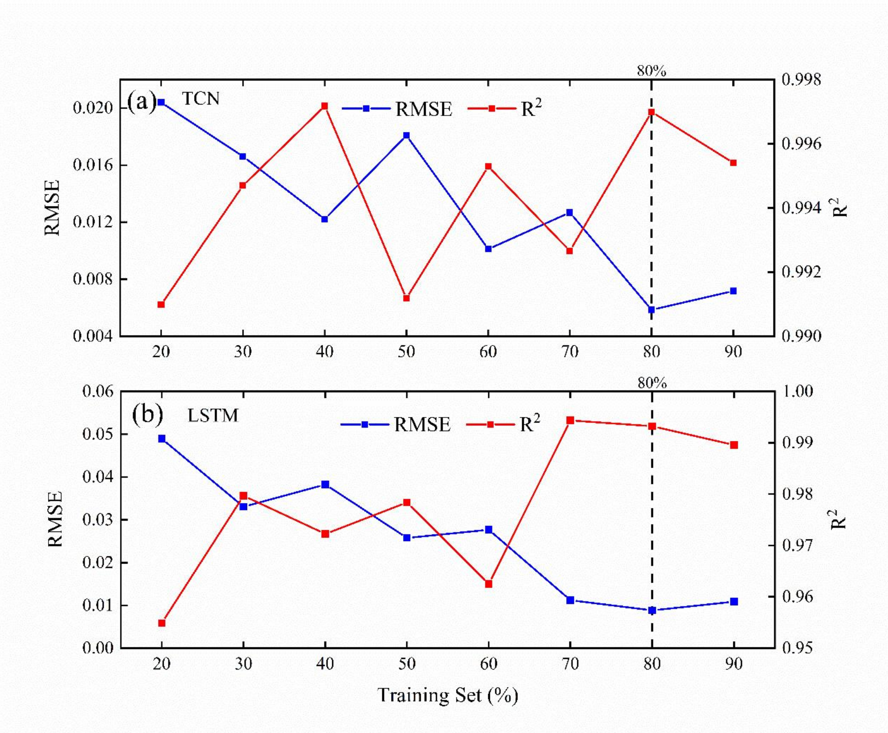

Figure 11. Influence of the percentage of training set on the performance of the model

5 Conclusions

A TCN-based deep learning model is proposed in this paper to predict groundwater levels in coastal aquifers. Hyper-parameter searches was first conducted and several different TCN-based models were tested to obtain a good architecture configuration. The results indicate that a deeper, broader model does not necessarily guarantee better predictions. The optimal configuration then were adopted for the networks of all monitoring data. This means that different data could share the same network architecture without adjusting in each case and broaden its application in different areas. With comparison to observations, the TCN-based model has achieved satisfactory performance on the prediction of groundwater levels, which can well

https://doi.org/10.5194/hess-2022-236
Preprint. Discussion started: 22 July 2022

capture the fluctuation of water level and provide possible saltwater intrusion information in the coastal area. Thus, it can be used as a new promising method for time-series prediction of hydrogeological data especially when the regional data is difficult to collect in a complex system.

To validate the newly developed TCN-based model, its performance is compared with the LSTM-based recurrent networks. The TCN-based model outperforms the LSTM-based model in view of both accuracy and efficiency. Meanwhile, three months ahead predictions were conducted with different leading periods. A decreasing precision is revealed when the leading time increases. In particular, once TCN was trained, due to the use of parallel convolution to process the input sequence, its prediction speed is significantly faster than recurrent networks. In summary, our research shows that TCN is a very powerful alternative to the LSTM network. It can provide accurate predictions and is suitable for more complex real-time applications because of its high efficiency.

Acknowledgements

This work was jointly supported by National Natural Science Foundation of China (No: 41702244), the Program for Jilin University (JLU) Science and Technology Innovative Research Team (No. 2019TD-35).

Code availability

The pieces of code that were used for all analyses are available from the authors upon request.

Data availability

https://doi.org/10.5194/hess-2022-236
Preprint. Discussion started: 22 July 2022

The data sets that have been analyzed in this paper are available from the authors upon request.

Author contribution

XZ drafted the manuscript and revised the manuscript. GC designed the experiments and collected all the data. DF developed the model code and performed the simulations. ZD was responsible for the project design, oversaw the analysis, and conducted manuscript revision as the project leader and the senior scientist.

Competing interests

The authors declare that they have no conflict of interest.

Reference

Abdalla, O. A. E., and Al-Rawahi, A. S.: Groundwater recharge dams in arid areas as tools for aquifer replenishment and mitigating seawater intrusion: example of AlKhod, Oman, Environ. Earth Sci., 69(6), 1951-1962, https://doi.org/10.1007/s12665-012-2028-x, 2012.

Baena-Ruiz, L., Pulido-Velazquez, D., Collados-Lara, A. J., Renau-Pruñonosa, A., and Morell, I.: Global Assessment of Seawater Intrusion Problems (Status and Vulnerability), Water Resour. Manag., 32(8), 2681-2700, https://doi.org/10.1007/s11269-018-1952-2, 2018.

Bai, S., Kolter, J. Z., and Koltun, V.: An Empirical Evaluation of Generic Convolutional and Recurrent Networks for Sequence Modeling, arXiv:1803.01271, https://doi.org/10.48550/arXiv.1803.01271, 2018.

Barlow, P. M., and Reichard, E. G.: Saltwater intrusion in coastal regions of North America, Hydrogeol. J., 18(1), 247-260, https://doi.org/10.1007/s10040-009-0514-3, 2009.

Batelaan, O., De Smedt, F., and Triest, L.: Regional groundwater discharge: phreatophyte mapping, groundwater modelling and impact analysis of

https://doi.org/10.5194/hess-2022-236
Preprint. Discussion started: 22 July 2022

land-use change, J. Hydrol., 275(1), 86-108, https://doi.org/10.1016/S0022-1694(03)00018-0, 2003.

Bengio, Y., Simard, P., and Frasconi, P.: Learning long-term dependencies with gradient descent is difficult, IEEE Trans. Neural Netw., 5(2), 157-166, https://doi.org/10.1109/72.279181, 1994.

Borovykh, A., Bohte, S., and Oosterlee, C. W.: Dilated convolutional neural networks for time series forecasting, J. Comput. Financ., 22(4), 73-101, https://doi.org/10.21314/JCF.2018.358, 2019.

Cannas, B., Fanni, A., See, L., and Sias, G.: Data preprocessing for river flow forecasting using neural networks: Wavelet transforms and data partitioning, Phys. Chem. Earth, Parts A/B/C, 31(18), 1164-1171, https://doi.org/10.1016/j.pce.2006.03.020, 2006.

Cao, Y., Ding, Y., Jia, M., and Tian, R.: A novel temporal convolutional network with residual self-attention mechanism for remaining useful life prediction of rolling bearings, Reliab. Eng. Syst. Saf., 215, https://doi.org/10.1016/j.ress.2021.107813, 2021.

Chen, Y., Kang, Y., Chen, Y., and Wang, Z.: Probabilistic forecasting with temporal convolutional neural network, Neurocomputing, 399, 491-501, https://doi.org/10.1016/j.neucom.2020.03.011, 2020.

Coulibaly, P., Anctil, F., Aravena, R., and Bobée, B.: Artificial neural network modeling of water table depth fluctuations, Water Resour. Res., 37(4), 885-896, https://doi.org/10.1029/2000WR900368, 2001.

Dai, Z., and Samper, J.: Inverse modeling of water flow and multicomponent reactive transport in coastal aquifer systems, J. Hydrol., 327(3-4), 447-461, https://doi.org/10.1016/j.jhydrol.2005.11.052, 2006.

Dai, Z., Xu, L, Xiao, T., McPherson, B., Zhang, X., Zheng, L., Dong, S., Yang, Z., Soltanian, M., Yang, C., Ampomah, W., Jia, W., Yin, S., Xu, T., Bacon, D., and Viswanathan, H.: Reactive chemical transport simulations of geologic carbon sequestration: Methods and applications, Earth-Sci. Rev., 208, 103265, https://doi.org/10.1016/j.earscirev.2020.103265, 2020.

https://doi.org/10.5194/hess-2022-236
Preprint. Discussion started: 22 July 2022

Danandeh Mehr, A., and Nourani, V.: A Pareto-optimal moving average-multigene genetic programming model for rainfall-runoff modelling, Environ. Modell. Softw., 92, 239-251, https://doi.org/10.1016/j.envsoft.2017.03.004, 2017.

Ergen, T., and Kozat, S. S.: Efficient Online Learning Algorithms Based on LSTM Neural Networks, IEEE Trans. Neural Netw. Learn. Syst., 29(8), 3772-3783, https://doi.org/10.1109/TNNLS.2017.2741598, 2018.

Feng, N., Geng, X., and Qin, L.: Study on MRI Medical Image Segmentation Technology Based on CNN-CRF Model, IEEE Access, 8, 60505-60514, https://doi.org/10.1109/ACCESS.2020.2982197, 2020.

Fischer, T., and Krauss, C.: Deep learning with long short-term memory networks for financial market predictions, Eur. J. Oper. Res., 270(2), 654-669, https://doi.org/10.1016/j.ejor.2017.11.054, 2018.

Gan, Z., Li, C., Zhou, J., and Tang, G.: Temporal convolutional networks interval prediction model for wind speed forecasting, Electr. Power Syst. Res., 191, 106865, https://doi.org/10.1016/j.epsr.2020.106865, 2021.

Garza-Díaz, L. E., DeVincentis, A. J., Sandoval-Solis, S., Azizipour, M., Ortiz-Partida, J. P., Mahlknecht, J., Cahn, M., Medellin-Azuara, J., ASCE, M., Zaccaria, D., and Kisekka, I.: Land-Use Optimization for Sustainable Agricultural Water Management in Pajaro Valley, California, J. Water Resour. Plan. Manage.-ASCE, 145(12), 5019018, https://doi.org/10.1061/(ASCE)WR.1943-5452.0001117, 2019.

Gorgij, A. D., Kisi, O., and Moghaddam, A. A.: Groundwater budget forecasting, using hybrid wavelet-ANN-GP modelling: A case study of Azarshahr Plain, East Azerbaijan, Iran, Hydrol. Res., 48(2), 455-467, https://doi.org/10.2166/nh.2016.202, 2017.

Han, D., Kohfahl, C., Song, X., Xiao, G., and Yang, J.: Geochemical and isotopic evidence for palaeo-seawater intrusion into the south coast aquifer of Laizhou Bay, China, Appl. Geochem., 26(5), 863-883, https://doi.org/10.1016/j.apgeochem.2011.02.007, 2011.

Han, D. M., Song, X. F., Currell, M. J., Yang, J. L., and Xiao, G. Q.: Chemical and isotopic constraints on evolution of groundwater salinization in the coastal plain aquifer of Laizhou Bay, China, J. Hydrol., 508, 12-27, https://doi.org/10.1016/j.jhydrol.2013.10.040, 2014.

He, K., Zhang, X., Ren, S., and Sun, J.: Deep Residual Learning for Image Recognition, In Proceedings of the IEEE conference on computer vision and pattern recognition, IEEE, pp. 770-778, https://doi.org/10.1109/CVPR.2016.90, 2016.

Huang, F. K., Chuang, M. H., Wang, G. S., and Yeh, H. D.: Tide-induced groundwater level fluctuation in a U-shaped coastal aquifer, J. Hydrol., 530, 291-305, https://doi.org/10.1016/j.jhydrol.2015.09.032, 2015.

Ketabchi, H., and Ataie-Ashtiani, B.: Evolutionary algorithms for the optimal management of coastal groundwater: A comparative study toward future challenges, J. Hydrol., 520, 193-213, https://doi.org/10.1016/j.jhydrol.2014.11.043, 2015.

Kingma, D. P., and Ba, J. L.: Adam: A method for stochastic optimization, 3rd International Conference on Learning Representations, San Diego, https://doi.org/10.48550/arXiv. 1412.16980, 2015.

Kratzert, F., Herrnegger, M., Klotz, D., Hochreiter, S., and Klambauer, G.: NeuralHydrology - Interpreting LSTMs in Hydrology, N/A, 11700, 347-362, https://doi.org/10.1007/978-3-030-28954-6-19, 2019.

Kreyenberg, P. J., Bauser, H. H., and Roth, K.: Velocity Field Estimation on Density - Driven Solute Transport with a Convolutional Neural Network, Water Resour. Res., 55(8), 7275-7293, https://doi.org/10.1029/2019WR024833, 2019.

Kumar Dubey, A., Kumar, A., García-Díaz, V., Kumar Sharma, A., and Kanhaiya, K.: Study and analysis of SARIMA and LSTM in forecasting time series data, Sustain. Energy Technol. Assess., 47, https://doi.org/10.1016/j.seta.2021.101474, 2021.

Lara-Benítez, P., Carranza-García, M., Luna-Romera, J. M., and Riquelme, J. C.: Temporal Convolutional Networks Applied to Energy-Related Time Series

Forecasting, Applied Sciences, 10(7), https://doi.org/10.3390/app10072322, 2020.

Lea, C., Flynn, M. D., Vidal, R., Reiter, A., and Hager, G. D.: Temporal convolutional networks for action segmentation and detection, Proceedings - 30th IEEE Conference on Computer Vision and Pattern Recognition, CVPR 2017, pp. 1003-1012, https://doi.org/10.1109/CVPR.2017.113, 2017.

Lea, C., Vidal, R., Reiter, A., and Hager, G. D.: Temporal convolutional networks: A unified approach to action segmentation, Lecture Notes in Computer Science (including subseries Lecture Notes in Artificial Intelligence and Lecture Notes in Bioinformatics). pp. 47-54, https://doi.org/10.1007/978-3-319-49409-8-7, 2016.

Lecun, Y., Bottou, L., Bengio, Y., and Haffner, P.: Gradient-based learning applied to document recognition, Proc. IEEE, 86(11), 2278-2324, https://doi.org/10.1109/5.726791, 1998.

Li, H., Jiao, J. J., Luk, M., and Cheung, K.: Tide-induced groundwater level fluctuation in coastal aquifers bounded by L-shaped coastlines, Water Resour. Res., 38(3), 6-6-8, https://doi.org/10.1029/2001WR000556, 2002.

Long, J., Shelhamer, E., and Darrell, T.: Fully convolutional networks for semantic segmentation, CVPR, pp. 431-440, https://doi.org/10.1109/CVPR.2015.7298965, 2015.

Lu, C. H., Cao, H. F., Ma, J., Shi, W. L., Rathore, S. S., Wu, J. C., and Luo, J.: A Proof - of - Concept Study of Using a Less Permeable Slice Along the Shoreline to Increase Fresh Groundwater Storage of Oceanic Islands: Analytical and Experimental Validation, Water Resour. Res., 55(8), 6450-6463, https://doi.org/10.1029/2018wr024529, 2019.

Maier, H. R., and Dandy, G. C.: Neural networks for the prediction and forecasting of water resources variables: a review of modelling issues and applications, Environ. Modell. Softw., 15(1), 101-124, https://doi.org/10.1016/S1364-8152(99)00007-9, 2000.

Mei, Y., Tan, G., and Liu, Z.: An improved brain-inspired emotional learning algorithm for fast classification, Algorithms, 10(2), 70, https://doi.org/10.3390/a10020070, 2017.

Nair, V., and Hinton, G. E.: Rectified linear units improve Restricted Boltzmann machines, In Proceedings of the 27th International Conference on International Conference on Machine Learning, pp. 807-814, https://dl.acm.org/doi/10.5555/3104322.3104425, 2010.

Park, Y., Lee, J. Y., Kim, J. H., and Song, S. H.: National scale evaluation of groundwater chemistry in Korea coastal aquifers: evidences of seawater intrusion, Environ. Earth Sci., 66(3), 707-718, https://doi.org/10.1007/s12665-011-1278-3, 2011.

Pascanu, R., Mikolov, T., and Bengio, Y.: On the difficulty of training recurrent neural networks, Machine Learning, pp. 2347-2355, https://doi.org/10.48550/arXiv.1211.5063, 2012.

Pratheepa, V., Ramesh, S., Sukumaran, N., and Murugesan, A. G.: Identification of the sources for groundwater salinization in the coastal aquifers of Southern Tamil Nadu, India, Environ. Earth Sci., 74(4), 2819-2829, https://doi.org/10.1007/s12665-015-4303-0, 2015.

Rumelhart, D. E., Hinton, G. E., and Williams, R. J.: Learning representations by back-propagating errors, Nature, 323(6088), 533-536, https://doi.org/10.1038/323533a0, 1986.

Sahoo, S., Russo, T. A., Elliott, J., Foster, I., and Argonne National Lab, A. I. L.: Machine learning algorithms for modeling groundwater level changes in agricultural regions of the U.S, Water Resour. Res., 53(5), 3878-3895, https://doi.org/10.1002/2016WR019933, 2017.

Salimans, T., and Kingma, D. P.: Weight normalization: A simple reparameterization to accelerate training of deep neural networks, Advances in Neural Information Processing Systems, pp. 901-909, https://doi.org/10.48550/arXiv.1602.07868, 2016.

Senthil Kumar, A. R., Sudheer, K. P., Jain, S. K., and Agarwal, P. K.: Rainfall-runoff modelling using artificial neural networks: comparison of network types,

https://doi.org/10.5194/hess-2022-236
Preprint. Discussion started: 22 July 2022

Hydrol. Process., 19(6), 1277-1291, https://doi.org/10.1002/hyp.5581, 2005.

Seo, Y., Kim, S., Kisi, O., and Singh, V. P.: Daily water level forecasting using wavelet decomposition and artificial intelligence techniques, J. Hydrol., 520, 224-243, https://doi.org/10.1016/j.jhydrol.2014.11.050, 2015.

Solgi, R., Loáiciga, H. A., and Kram, M.: Long short-term memory neural network (LSTM-NN) for aquifer level time series forecasting using in-situ piezometric observations, J. Hydrol., 601, https://doi.org/10.1016/j.jhydrol.2021.126800, 2021.

Srivastava, N., Hinton, G., Krizhevsky, A., Sutskever, I., and Salakhutdinov, R.: Dropout: A simple way to prevent neural networks from overfitting, J. Mach. Learn. Res., 15(1), 1929-1958, https://dl.acm.org/doi/abs/10.5555/2627435.2670313, 2014.

Taylor, K. E.: Summarizing multiple aspects of model performance in a single diagram, J. Geophys. Res.-Atmos., 106, 7183-7192, https://doi.org/10.1029/2000JD900719, 2001.

Torres, J. F., Troncoso, A., Koprinska, I., Wang, Z., and Martínez-Álvarez, F.: Deep Learning for Big Data Time Series Forecasting Applied to Solar Power, The 13th International Conference on Soft Computing Models in Industrial and Environmental Applications, pp. 123-133, https://doi.org/10.1007/978-3-319-94120-2_12, 2018.

Wan, R., Mei, S., Wang, J., Liu, M., and Yang, F.: Multivariate temporal convolutional network: A deep neural networks approach for multivariate time series forecasting, Electronics, 8(8), https://doi.org/10.3390/electronics8080876, 2019.

Wunsch, A., Liesch, T., and Broda, S.: Groundwater level forecasting with artificial neural networks: a comparison of long short-term memory (LSTM), convolutional neural networks (CNNs), and non-linear autoregressive networks with exogenous input (NARX), Hydrol. Earth Syst. Sci., 25(3), 1671-1687, https://doi.org/10.5194/hess-25-1671-2021, 2021.

Xu, Z., and Hu, B.X.: Development of a discrete-continuum VDFST-CFP numerical

https://doi.org/10.5194/hess-2022-236
Preprint. Discussion started: 22 July 2022

model for simulating seawater intrusion to a coastal karst aquifer with a conduit system, Water Resour. Res., 53(1), 688-711, https://doi.org/10.1002/2016wr018758, 2017.

Xue, Y., Wu, J., Ye, S., and Zhang, Y.: Hydrogeological and hydrogeochemical studies for salt water intrusion on the south coast of Laizhou Bay, China, Groundwater, 38(1), 38-45, https://doi.org/10.1111/j.1745-6584.2000.tb00200.x, 2000.

Yan, J., Mu, L., Wang, L., Ranjan, R., and Zomaya, A. Y.: Temporal Convolutional Networks for the Advance Prediction of ENSO, Sci Rep., 10(1), 8055-8055, https://doi.org/10.1038/s41598-020-65070-5, 2020.

Zeng, X., Wu, J., Wang, D., and Zhu, X.: Assessing the pollution risk of a groundwater source field at western Laizhou Bay under seawater intrusion, Environ. Res., 148, 586-594, https://doi.org/10.1016/j.envres.2015.11.022, 2016.

Zhan, C., Dai, Z., Soltanian, M. R., and Zhang, X.: Stage - wise stochastic deep learning inversion framework for subsurface sedimentary structure identification, Geophys. Res. Lett., 49(1), e2021GL095823, https://doi.org/10.1029/2021GL095823, 2022.

Zhang, D., Lin, J. Q., Peng, Q. D., Wang, D. S., Yang, T. T., Sorooshian, S., Liu, X. F., and Zhuang, J. B.: Modeling and simulating of reservoir operation using the artificial neural network, support vector regression, deep learning algorithm, J. Hydrol., 565, 720-736, https://doi.org/10.1016/j.jhydrol.2018.08.050, 2018a.

Zhang, J., Zhang, X. Y., Niu, J., Hu, B. X., Soltanian, M. R., Qiu, H., and Yang, L.: Prediction of groundwater level in seashore reclaimed land using wavelet and artificial neural network-based hybrid model, J. Hydrol., 577, 123948, https://doi.org/10.1016/j.jhydrol.2019.123948, 2019.

Zhang, J., Zhu, Y., Zhang, X., Ye, M., and Yang, J.: Developing a Long Short-Term Memory (LSTM) based model for predicting water table depth in agricultural areas, J. Hydrol., 561, 918-929, https://doi.org/10.1016/j.jhydrol.2018.04.065,

https://doi.org/10.5194/hess-2022-236
Preprint. Discussion started: 22 July 2022

2018b.

Zhang, X. Y., Dong, F., Dai, H., Hu, B. X., Qin, G. X., Li, D., Lv, X. S., Dai, Z. X., and Soltanian, M. R.: Influence of lunar semidiurnal tides on groundwater dynamics in estuarine aquifers, Hydrogeol. J., 28(4), 1419-1429, https://doi.org/10.1007/s10040-020-02136-8, 2020.

Zhang, X. Y., Miao, J. J., Hu, B. X., Liu, H. W., Zhang, H, X., and Ma, Z.: Hydrogeochemical characterization and groundwater quality assessment in intruded coastal brine aquifers (Laizhou Bay, China), Environ. Sci. Pollut. Res., 24(26), 21073-21090, https://doi.org/10.1007/s11356-017-9641-x, 2017.